

Shear Bernstein modes in a two-dimensional electron liquid

A. N. Afanasiev* and P. S. Alekseev, A. A. Greshnov, M. A. Semina
Ioffe Institute, St. Petersburg 194021, Russia

Bernstein modes are formed as a result of non-local coupling of collective excitations and cyclotron harmonics in magnetized plasma. In degenerate solid state plasma they are typically associated with magnetoplasmons. A different type of Bernstein modes arises in two-dimensional electron liquid at sufficiently strong quasiparticle interaction. We consider Bernstein modes originating from coupling between quasiparticle cyclotron harmonics and shear magnetosound waves. The latter may be responsible for the giant peak in radio-frequency photoresistance observed in high-quality GaAs quantum wells. Using Landau-Silin kinetic equation with an arbitrary strength of the interparticle Landau interaction, we trace the reconstruction of Bernstein mode spectrum in high-quality 2D electron systems across the crossover between weakly interacting degenerate electron gas and the correlated electron liquid. Sensitivity of Bernstein modes to the strength of quasiparticle interaction allows one to use them for spectroscopy of Landau interaction function in the electron Fermi liquids.

I. INTRODUCTION

Recent demonstration of hydrodynamic electron transport [1, 2] in ultrapure samples of graphene [3–7], 2D metals [8, 9] and semiconductor heterostructures [10–13] has marked the practical realization of pristine two-dimensional electron liquid (2DEL), which dynamics is governed solely by the electron-electron interaction while the effects of disorder and electron-phonon interaction are very minor. Experimental studies of high-frequency response of hydrodynamic samples, namely their photoresistance in classically strong magnetic fields, revealed non-sinusoidal shape of microwave-induced resistance oscillations (MIRO) [14–17] and abnormally strong absorption at cyclotron resonance overtones [15–19]. The latter effect is especially pronounced in GaAs quantum wells at the second cyclotron harmonic [15–17, 19].

High-frequency properties of electron liquid are typically associated with the collisionless collective modes [20, 21], and the effect of giant photoresponse was attributed to excitation of the two different types of waves. First of them [18, 22, 23] are Bernstein modes (BMs) [24, 25] in 2D degenerate electron gas (2DEG) [26, 27]. At the wave vectors comparable to the inverse cyclotron radius, magnetoplasmon and single particle excitations are coupled due to non-uniformity of the self-consistent electrostatic field of the wave at the cyclotron orbit. As a result, long wavelength magnetoplasmon dispersion splits into series of BM branches between the sequential cyclotron harmonics.

The second explanation [28, 29] of the giant photoresponse relies on viscoelasticity of 2DEL [30]. At sufficiently high frequencies, $\omega \gg \nu_2$ (here ν_2 is the inverse shear stress relaxation time determined by the electron-electron collisions), the viscosity coefficient becomes purely imaginary and proportional to the elastic shear modulus. Behavior of the electron liquid is similar to amorphous solid in this frequency domain: shear

stress density $\hat{\Pi}_{\text{sh}}(\mathbf{r}, t)$ oscillates in phase with particle current density $\mathbf{j}(\mathbf{r}, t)$ and thus can propagate in the form of shear sound, in contrast to attenuation in hydrodynamic regime $\omega \ll \nu_2$ [31]. From the microscopic point of view, shear wave in electron liquid is represented by transverse zero sound [32]. It emerges in 2DEL with relatively strong dipole part of the short-range Landau interaction, when quasiparticle mass $m = (1 + F_1)m^{(0)}$ [33] exceeds the threshold value of $2m^{(0)}$ [34–36] (here F_1 is the spin-symmetric dipole Landau parameter and $m^{(0)}$ is the effective electron mass before the interaction is turned on). The required degree of mass renormalization has been observed in high purity semiconductor heterostructures with low carrier concentration [37–43].

In external magnetic field, shear stress density is determined by the two viscosity coefficients: ordinary (even) $\eta_s(\omega)$ and Hall (odd) $\eta_H(\omega)$ [44, 45], both having resonance at the renormalized second cyclotron harmonic [46]. This viscoelastic resonance manifests itself via reconstruction of the collective excitation spectrum at long wavelengths. Besides the conventional magnetoplasmon, spectrum consists of the shear magnetosound mode [28, 29], which leads to the giant peak in photoresistance at the second cyclotron harmonic [15–17, 19, 28, 47]. However, the viscoelastic model is valid [29] only in the long wavelength domain for strongly-interacting 2DEL, while the quasiparticle interaction strength is arbitrary and dependent on r_s in realistic GaAs structures.

In this Letter we consider the evolution of collective mode spectrum of magnetized 2DEL with the increase of quasiparticle interaction strength. Using Landau-Silin kinetic equation [20, 21, 48] we show that the conventional BM pattern of 2DEG is reconstructed at strong quasiparticle mass renormalization (high F_1). The emergent shear magnetosound mode couples with the quasiparticle excitations and forms another type of BMs. Renormalized second cyclotron resonance harmonic becomes the main one and the resulting collective excitation spectrum consists of the two independent series of BMs. The *conventional BMs* are related to magnetoplasmon and characterized by the longitudinal current polarization, while the coexisting *shear BMs* related to shear

* afanasiev.an@mail.ru

magneto-sound carry the transverse current density.

II. LONG WAVELENGTH EXCITATIONS IN MAGNETIZED VISCOELASTIC 2DEL

Single-particle excitations of magnetized 2DEL are represented by quasiparticle transitions to higher Landau levels above the topmost occupied one in the ground state. At large filling factors, they are characterized by harmonics of the renormalized cyclotron frequency $\omega_c = eH/mc$ [33] and the wave packets describing the excited quasiparticles are localized at circular orbits with cyclotron radius $R_c = v_F/\omega_c$ up to the Fermi wavelength (here v_F is the Fermi velocity). In contrast to the weakly-interacting 2DEG case, long wavelength cyclotron resonance frequencies $\bar{\omega}_n$ in magnetized 2DEL differ from the quasiparticle cyclotron harmonics $n\omega_c$. In 2DEL, local cyclotron rotation of macroscopic quantities proportional to the angular harmonics of non-equilibrium distribution function (e.g. current and shear stress densities) is affected by quasiparticle backflow [20] caused by the short-range interaction. As a result, the rotation frequency associated with the n -th angular harmonic undergoes additional renormalization [21, 49] and is given by $\bar{\omega}_n = n(1 + F_n)\omega_c$. In particular, current density rotates with the bare frequency $\bar{\omega}_1 = eH/m^{(0)}c$ (main cyclotron resonance harmonic) in consistence with Kohn's theorem [50] and the shear stress rotation is governed by $\bar{\omega}_2 = 2(1 + F_2)\omega_c$, see Fig. 1a.

To describe the collective modes of 2DEL in magnetic field within the viscoelastic model we combine the linearized Navier-Stokes and continuity equations for the non-equilibrium quasiparticle density $\delta N(\mathbf{r}, t)$ and current density $\mathbf{j}(\mathbf{r}, t)$. For the waves propagating along Ox with the wave vector q at frequency ω , the set of equations for the Fourier transformed quantities $\delta N_{\omega q}$, $\mathbf{j}_{\omega q}$ reads

$$-i\omega\delta N + iqj_x = 0, \quad (1)$$

$$[-i\omega + \bar{\nu}_1 + \eta_s(\omega)q^2]j_x = [\bar{\omega}_1 + \eta_H(\omega)q^2]j_y - iq_s^2(q)\delta N, \quad (2)$$

$$[-i\omega + \bar{\nu}_1 + \eta_s(\omega)q^2]j_y = -[\bar{\omega}_1 + \eta_H(\omega)q^2]j_x. \quad (3)$$

Here $\bar{\nu}_n = (1 + F_n)\tau_n^{-1}$ denote renormalized effective scattering rates [20], and $\bar{\nu}_1 \ll \bar{\nu}_2$ describes momentum relaxation due to scattering by disorder. The Eqs. (1)-(3) valid at strong dipole Landau interaction $F_1 \gg 1$ [29] and $qR_c \ll 1$ determine the long wavelength dispersion of the two types of waves in viscoelastic 2DEL. The last term in (2) describes restoring force for the charge density oscillations due to quasiparticle compressibility and long-range self-consistent electrostatic field $U(\mathbf{r}, t) = \int V(|\mathbf{r} - \mathbf{r}'|)\delta N(\mathbf{r}', t)d\mathbf{r}'$. Here $V(r)$ is the 2D Coulomb interaction screened by metallic gate introduced to a 2D sample to control the carrier concentration, its Fourier transform is $V(q) = \frac{2\pi e^2}{\kappa q}(1 - e^{-2qd})$, where κ is the static

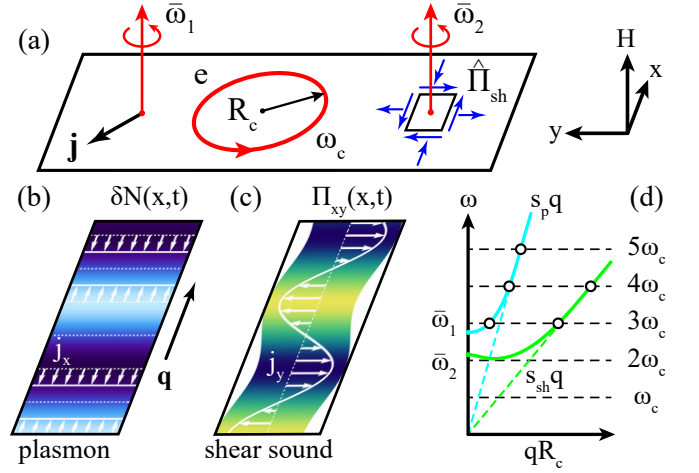


FIG. 1. Formation of Bernstein modes in 2DEL with strong dipole quasiparticle interaction; a) cyclotron rotation of current density, shear stress density and individual quasiparticles (marked by red circles) in magnetic field; b) and c) propagation of plasmon and shear sound in 2DEL: quasiparticle and shear stress densities in the waves are marked by color, white arrows denote current density fields, shape of the colored region correspond to the typical displacement of the finite liquid element under wave propagation; d) long wavelength dispersions of magnetoplasmon (cyan) and shear magnetosound (light green) in gated 2DEL and their counterparts at zero magnetic field (dashed lines), white circles mark the positions of anti-crossings with single particle excitations at $n\omega_c$ leading to Bernstein modes.

background dielectric constant and d is the distance between the gate and 2DEL. At zero magnetic field, dispersion of *longitudinal* (see Fig. 1b) plasmon wave $\omega_p(q) = s_p(q)q$ in 2D and its velocity $s_p^2(q) = (1 + F_1)(1 + \tilde{F}_0)v_F^2/2$ are determined by the renormalized [20, 48, 49] Landau parameters $\tilde{F}_n(q) = F_n + F_c(q)\delta_{n0}$ which describe total quasiparticle interaction in the n -channel consisting of short-range F_n and Coulomb $F_c(q) = DV(q)$ parts (here D stands for the 2D density of states). In magnetic field, plasmons are hybridized with current cyclotron rotation leading to magnetoplasmon with dispersion

$$\omega_{\text{mp}}(q) = \sqrt{\bar{\omega}_1^2 + \omega_p^2(q)}. \quad (4)$$

Frequency-dependent kinematic shear viscosity coefficients given by

$$\eta_s(\omega) = i(1 + F_1)(1 + F_2)\frac{v_F^2}{4}\frac{\omega + i\bar{\nu}_2}{(\omega + i\bar{\nu}_2)^2 - \bar{\omega}_2^2}, \quad (5)$$

$$\eta_H(\omega) = (1 + F_1)(1 + F_2)\frac{v_F^2}{4}\frac{\bar{\omega}_2}{(\omega + i\bar{\nu}_2)^2 - \bar{\omega}_2^2}, \quad (6)$$

describe viscoelasticity of magnetized 2DEL. In classically weak magnetic fields $\bar{\omega}_2\tau_2 \ll 1$, viscoelastic properties of 2DEL are similar to the zero field case: Hall (odd) viscosity $\eta_H(\omega)$ is negligible and the ordinary (even) shear viscosity $\eta_s(\omega)$ becomes purely imaginary

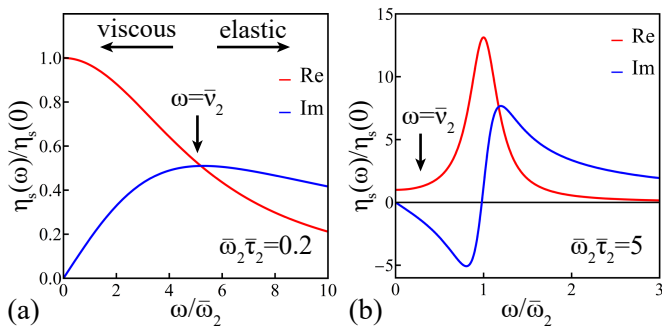


FIG. 2. Viscoelasticity of 2DEL in a) weak and b) strong magnetic fields; $\bar{\omega}_2 = 2(1 + F_2)\omega_c$ and $\bar{\nu}_2 = \bar{\tau}_2^{-1} = (1 + F_2)\nu_2$ denote renormalized frequencies of the shear stress cyclotron rotation and relaxation, respectively.

in collisionless domain $\omega\bar{\tau}_2 \gg 1$ (see Fig. 2a), enabling propagation of the shear sound with linear dispersion $\omega_{\text{sh}}(q) = s_{\text{sh}}q$. Its velocity $s_{\text{sh}}^2 = (1 + F_1)(1 + F_2)v_F^2/4$ coincides with the velocity of transverse zero sound [32] in 2D [34] within the applicability domain of the viscoelastic model ($F_1 \gg 1$). In contrast to compression (plasmon) wave, quasiparticle density in *transverse* shear sound remains constant, hence its dispersion is unaffected by Coulomb interaction. Due to oscillations of non-diagonal components of the shear stress tensor $\Pi_{xy}(x, t)$ in the wave, each element of the electron liquid is deformed in direction perpendicular to the wave vector without volume change (see Fig. 1c). At classically strong magnetic fields $\bar{\omega}_2\bar{\tau}_2 \ll 1$, viscous behavior is reestablished (see Fig. 2b) in the part of the collisionless domain near the shear stress cyclotron rotation frequency $\bar{\omega}_2$ (see Fig. 1a). This viscoelastic resonance appearing in both $\eta_s(\omega)$ and $\eta_H(\omega)$ leads to shear magnetosound mode, representing the second solution of the system (1)-(3). Its dispersion starts at the second cyclotron resonance harmonic $\omega_{\text{ms}}(0) = \bar{\omega}_2$ and has two characteristic parts depending on the ratio $\bar{\omega}_1/\omega_p$,

$$\omega_{\text{ms}}(q) = \begin{cases} \sqrt{\bar{\omega}_2^2 - 2\bar{\omega}_2\omega_{\text{sh}}^2/\bar{\omega}_1 + \omega_p^2\omega_{\text{sh}}^2/\bar{\omega}_1^2}, & \bar{\omega}_1 \gg \omega_p \\ \sqrt{\bar{\omega}_2^2 + \omega_{\text{sh}}^2}, & \bar{\omega}_1 \ll \omega_p. \end{cases} \quad (7)$$

Eq. (7) is obtained using the relations $\bar{\omega}_2 \ll \bar{\omega}_1$ and $\omega_{\text{sh}} \ll \omega_p$ between characteristic frequencies of the viscoelastic model (provided $\tilde{F}_0, F_1 \gg 1$). At $\bar{\omega}_1/\omega_p \gg 1$, longitudinal (in current polarization) plasmon and transverse shear oscillations are mixed by the circularly polarized cyclotron motion. The corresponding dispersion is characterized by negative wave velocity at small q due to Hall viscosity. This effect is similar for hydrodynamic waves in neutral fluids [10]. At $\bar{\omega}_1/\omega_p \ll 1$, plasmon and shear waves are separated and dispersion equation takes the form $\omega = -i\eta_s q^2$ conventional for the shear sound, but with modified viscosity (5). The dispersion $\omega_{\text{ms}}(q)$ in this limit was obtained in [28, 29].

Both magnetoplasmon and shear magnetosound are

longitudinal (with respect to self-consistent field) electrostatic modes in magnetized 2DEL. Their dispersion laws can be found from zeros of the longitudinal dielectric function $\varepsilon_{xx}(\omega, \mathbf{q}) = 0$ calculated using Eqs. (1)-(3), while the poles of $\varepsilon_{yy}(\omega, \mathbf{q})$ responsible for transverse modes are absent. At short wavelengths $qR_c \sim 1$, magnetoplasmon is coupled to quasiparticle cyclotron harmonics near their crossing points (see Fig. 1d), leading to formation of the conventional BMs. Longitudinal shear magnetosound generates a different type of BMs via the same mechanism. Since the threshold of the shear sound emergence in 2D $F_1 \geq 1$ coincides (at $F_n = 0$ for $|n| \geq 2$) with *inversion* of the main and the second cyclotron resonance harmonics $\bar{\omega}_2 \leq \bar{\omega}_1$ (see Fig. 1d), magnetoplasmon and shear magnetosound dispersions do not cross and the latter forms its own series of BMs independently.

III. BERNSTEIN MODES IN 2DEL

To obtain dispersion of BMs in 2DEL we go beyond the viscoelastic model and use Landau-Silin kinetic equation [20, 21, 48] valid in the quasiclassical domain at arbitrary strength of the short-range interaction. Its linearized form is

$$\partial_t \delta n + [\mathbf{v}_F \nabla + \omega_c \partial_\theta] \delta \bar{n} - \mathbf{v}_F [\nabla U + e \mathbf{E}_0] n'_0 = \text{St}[\delta \bar{n}], \quad (8)$$

where \mathbf{E}_0 is the external electric field, θ is the angle between quasiparticle velocity at the Fermi surface and Ox (the geometry is shown in Fig. 1). Here $\delta n_{\mathbf{p}}(\mathbf{r}, t)$ stands for the global non-equilibrium part of distribution function, $\delta \bar{n}_{\mathbf{p}}(\mathbf{r}, t) = n_{\mathbf{p}}(\mathbf{r}, t) - n_0(\tilde{\mathcal{E}}_{\mathbf{p}}(\mathbf{r}, t))$ describes deviation from the local equilibrium [20] characterized by the local energy of quasiparticle $\tilde{\mathcal{E}}_{\mathbf{p}}(\mathbf{r}, t) = \epsilon(\mathbf{p}) + \delta \mathcal{E}_{\mathbf{p}}(\mathbf{r}, t)$ consisting of the non-interacting part $\epsilon(\mathbf{p}) = p^2/2m$ and the contribution from Landau short-range interaction $\delta \mathcal{E}_{\mathbf{p}}(\mathbf{r}, t) = \sum_{\mathbf{p}'} f_s(\widehat{\mathbf{p}\mathbf{p}'}) \delta n_{\mathbf{p}'}(\mathbf{r}, t)$. We describe weakly excited state of 2DEL in terms of the small Fermi surface deformation $\Phi(\theta, \mathbf{r}, t) \ll \mu$ related to the distribution function via $\delta n_{\mathbf{p}}(\mathbf{r}, t) = -n'_0(\epsilon) \Phi(\theta, \mathbf{r}, t)$, where $n_0(\epsilon) = \Theta(\mu - \epsilon)$ is the equilibrium distribution and μ is the Fermi energy.

We consider plane-wave like ($\mathbf{q} \parallel Ox$) solutions $\Phi(\theta, \mathbf{r}, t) = \Phi(\theta) e^{i(\mathbf{q}\mathbf{r} - \omega t)}$ of the homogeneous form of kinetic equation (8) in collisionless regime, thus we omit the collision integral $\text{St}[\delta \bar{n}]$ everywhere, except for regularization of singularities. Expanding Fermi surface deformation $\Phi(\theta) = \sum_n \Phi_n e^{in\theta}$ and spin-symmetric part of the Landau interaction function $f_s(\widehat{\mathbf{p}_F \mathbf{p}'_F}) = D^{-1} \sum_n F_n e^{in(\theta - \theta')}$ in Fourier series (note that $F_n = F_{-n}$) and combining them with Eq. (8), we obtain closed system for the angular harmonics of $\Phi(\theta)$

$$(1 + \tilde{F}_n) \Phi_n - \sum_s A_{ns} \tilde{F}_s \Phi_s = 0, \quad (9)$$

$$A_{ns}(\Omega, k) = \Omega \sum_l \frac{J_{l-n}(k) J_{l-s}(k)}{\Omega - l + i\gamma}, \quad (10)$$

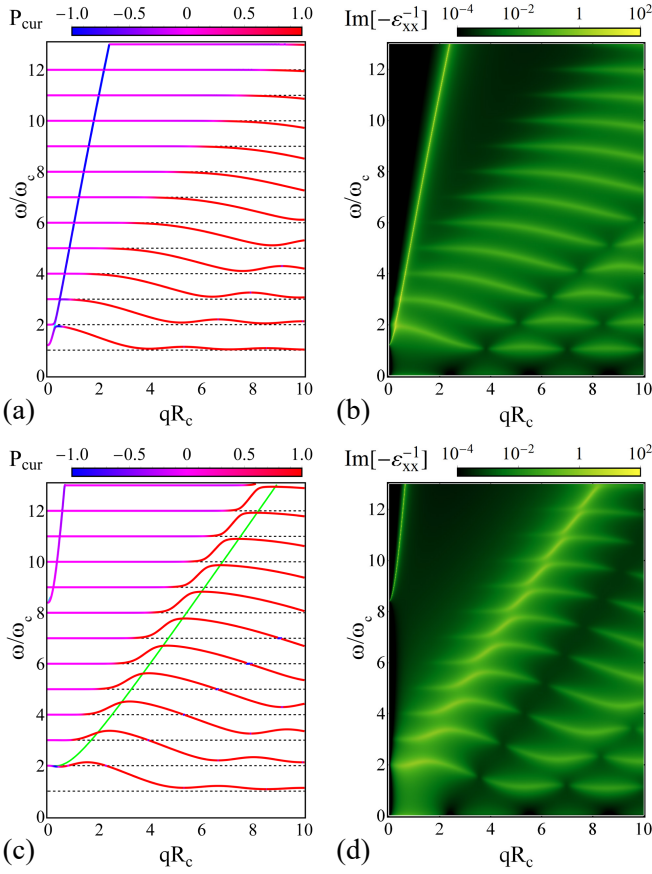


FIG. 3. Bernstein modes spectrum (a,c) and its visualization through the energy loss function (b,d) in gated 2DEL with $R_c/a_B = 300$, $d/R_c = 0.1$ for weak $F_0 = -0.4$, $F_1 = 0.2$ (a,b) and strong $F_0 = -2$, $F_1 = 7.4$ (c,d) dipole Landau interaction at $\gamma = 0.1$. Color of the dispersion curves in a) and c) show linear current polarization degree. Cyan and light green curves denote long wavelength dispersions of magnetoplasmon and shear magnetosound, respectively.

where $\Omega = \omega/\omega_c$ and $k = qR_c$ are the dimensionless frequency and wave vector, $J_n(k)$ is the Bessel function of the first kind and $\gamma = \nu_{ee}/\omega_c$ stands for the dimensionless quasiparticle scattering rate appearing in the model collision integral $\text{St}[\delta\bar{n}] = n_0\nu_{ee} \sum_{|n|\geq 2} \Phi_n e^{in\theta}$, which we use in this work. At zero wave vector, the solutions of Eq. (9) are $\text{Re}\omega(0) = \bar{\omega}_n$.

In this work, we consider the effect of short-range interaction in isotropic and dipole channels only [32, 34–36, 49, 51, 52], thus the system (9) reduces to

$$\begin{bmatrix} 1 - \beta A_{11}^+ & -\tilde{F}_0 A_{10} & 1 - \beta A_{11}^- \\ -\beta A_{01}^+ & 1 + \tilde{F}_0(1 - A_{00}) & -\beta A_{01}^- \\ 1 - \beta A_{11}^+ & -\tilde{F}_0 A_{10} & -1 + \beta A_{11}^- \end{bmatrix} \begin{bmatrix} j_x \\ v_F \delta N \\ ij_y \end{bmatrix} = 0, \quad (11)$$

where $A_{ns}^\pm = A_{ns} \pm A_{n\bar{s}}$, $\bar{s} = -s$, $\beta = F_1/(1 + F_1)$ and non-equilibrium quasiparticle and current densities are given by $\delta N(\mathbf{r}, t) = 2 \sum_{\mathbf{p}} \delta n_{\mathbf{p}}(\mathbf{r}, t)$ and $\mathbf{j}(\mathbf{r}, t) = 2 \sum_{\mathbf{p}} \mathbf{v}_{\mathbf{p}} \delta \bar{n}_{\mathbf{p}}(\mathbf{r}, t)$. Eqs. (11) are analogous to macro-

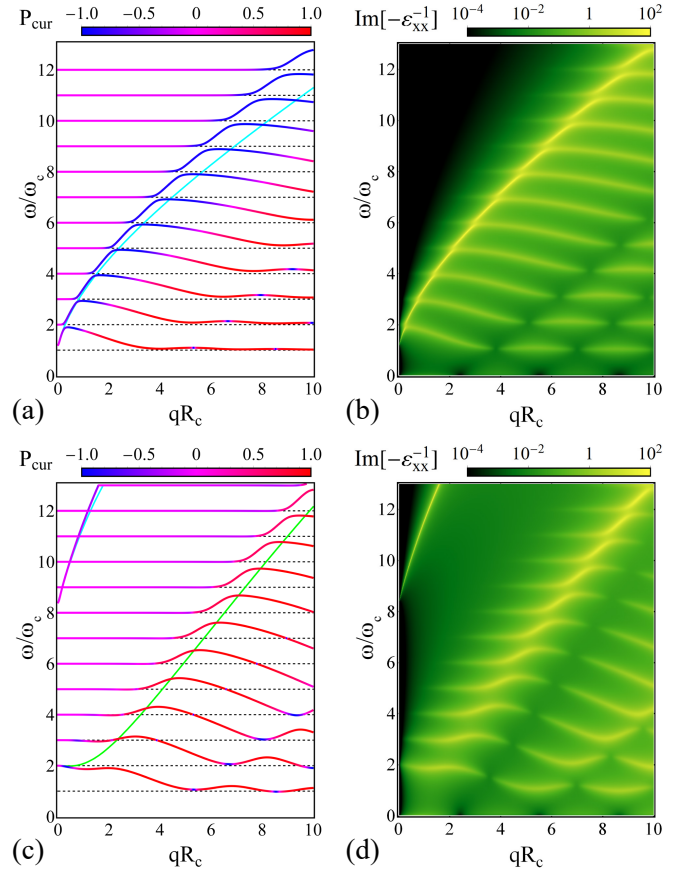


FIG. 4. Bernstein modes spectrum (a,c) and its visualization through the energy loss function (b,d) in ungated 2DEL with $R_c/a_B = 15$, $d/R_c = 10$, for weak $F_0 = -0.4$, $F_1 = 0.2$ (a,b) and strong $F_0 = -2$, $F_1 = 7.4$ (c,d) dipole Landau interaction at $\gamma = 0.1$. Other notations are the same as in Fig. 3.

scopic equations of the viscoelastic model (1)–(3) valid at short wavelengths and arbitrary short-range interaction strength. In 2DEL, isotropic Landau parameter F_0 is typically negative and decreases with r_s [53–55], while the dipole one F_1 is positive and increases with r_s [37–43].

The BM spectra of the gated and ungated 2DELs with either weak and strong dipole Landau interaction calculated after Eqs. (11) are shown in Fig. 3a,c and Fig. 4a,c, respectively. The color of the curves corresponding to the linear current polarization degree $P_{\text{cur}} = (|j_y|^2 - |j_x|^2)/(|j_y|^2 + |j_x|^2)$ visualizes nature of the modes (at particular q): 1) plasmon-like ($P_{\text{cur}} = -1$) with longitudinal current polarization, 2) shear wave like ($P_{\text{cur}} = 1$) carrying the transverse current or 3) cyclotron motion like ($P_{\text{cur}} = 0$) with circular current polarization. In the weakly interacting case (Figs. 3a and 4a) the conventional BM pattern is reproduced and the magnetoplasmon-like segments of dispersion are characterized by longitudinal current polarization. With the increase of F_1 , magnetoplasmon dispersion and the associated BMs are shifted upwards relative to quasiparticle harmonics. At strong dipole interaction, the calculated spectra (Figs. 3c

and 4c) demonstrate inversion of the main and the second cyclotron resonance harmonics and reconstruction of BM pattern regardless of the screening strength (induced by the gate). Shear BMs with transverse current polarization arise due to anti-crossings of shear magnetosound dispersion and quasiparticle cyclotron harmonics. In contrast to the conventional BM case, each branch of the new type spreads to a wider frequency range greater than ω_c .

In Fig. 3b,d and Fig. 4b,d we plot maps of the energy loss function $\text{Im}[-\varepsilon_{xx}^{-1}(\omega, \mathbf{q})]$ [20, 21] (determined by the longitudinal nonlocal proper conductivity calculated using the full kinetic equation (8)), which describes the inelastic scattering of high energy electrons passing through the system [56]. Positions of the peaks of $\text{Im}[-\varepsilon_{xx}^{-1}(\omega, \mathbf{q})]$ on the (ω, q) plane and their widths correspond to dispersion and damping of the longitudinal collective modes, respectively. It is well seen that the shear BMs are well-defined and directly accessible through the energy-loss techniques.

IV. CONCLUSIONS

In this work we have considered the emergence of shear BMs and inversion of the cyclotron resonance harmonics due to strong dipole Landau interaction. Sensitivity of BM spectrum to the short-range quasiparticle interaction can be used for spectroscopy of 2DEL. Inversion of the

cyclotron resonance frequencies and emergence of shear BMs can be treated as a hallmark of strong interaction in 2DEL. Similarly to the shear magnetosound [19, 28, 47], shear BMs can be excited in the ac magnetotransport experiments and may lead to the giant peak in photoresistance at second and higher cyclotron harmonics. The effect may be used for estimation of the anisotropic part of Landau interaction function at various r_s and magnetic fields, by analogy with the 3D metal case [21] where excitation of the cyclotron waves is involved. Interestingly, reconstruction of the BM spectrum can happen in higher angular channels at $F_n \gg 1$, and emergence of the modes associated with the corresponding zero sound branch (e.g. for quadrupole interaction see [49, 51, 57, 58]) is expected, as well as cyclotron resonance frequencies inversion with respect to the n -th harmonic $\bar{\omega}_n$.

ACKNOWLEDGMENTS

A.N.A. and P.S.A. are grateful to the Foundation for the Advancement of Theoretical Physics and Mathematics “BASIS” (Grant No. 23-1-2-25-2) for financial support of analytical calculations based on kinetic equation in Section 3. The work of A.N.A. (numerical calculations in Section 3) was supported by the Ministry of Science and Higher Education of the Russian Federation [project no. 075-15-2020-790].

-
- [1] M. Polini and A. K. Geim, Viscous electron fluids, *Physics Today* **73**, 28 (2020).
 - [2] B. N. Narozhny, Hydrodynamic approach to two-dimensional electron systems, *Riv. Nuovo Cim.* **45**, 661 (2022).
 - [3] D. A. Bandurin, I. Torre, R. K. Kumar, M. Ben Shalom, A. Tomadin, A. Principi, G. H. Auton, E. Khestanova, K. S. Novoselov, I. V. Grigorieva, L. A. Ponomarenko, A. K. Geim, and M. Polini, Negative local resistance caused by viscous electron backflow in graphene, *Science* **351**, 1055 (2016).
 - [4] J. Crossno, J. K. Shi, K. Wang, X. Liu, A. Harzheim, A. Lucas, S. Sachdev, P. Kim, T. Taniguchi, K. Watanabe, T. A. Ohki, and K. C. Fong, Observation of the Dirac fluid and the breakdown of the Wiedemann-Franz law in graphene, *Science* **351**, 1058 (2016).
 - [5] J. A. Sulpizio, L. Ella, A. Rozen, J. Birkbeck, D. J. Perello, D. Dutta, M. Ben-Shalom, T. Taniguchi, K. Watanabe, T. Holder, R. Queiroz, A. Principi, A. Stern, T. Scaffidi, A. K. Geim, and S. Ilani, Visualizing Poiseuille flow of hydrodynamic electrons, *Nature* **576**, 75 (2019).
 - [6] M. J. H. Ku, T. X. Zhou, Q. Li, Y. J. Shin, J. K. Shi, C. Burch, L. E. Anderson, A. T. Pierce, Y. Xie, A. Hamo, U. Vool, H. Zhang, F. Casola, T. Taniguchi, K. Watanabe, M. M. Fogler, P. Kim, A. Yacoby, and R. L. Walsworth, Imaging viscous flow of the Dirac fluid in graphene, *Nature* **583**, 537 (2019).
 - [7] C. Kumar, J. Birkbeck, J. A. Sulpizio, D. Perello, T. Taniguchi, K. Watanabe, O. Reuven, T. Scaffidi, A. Stern, A. K. Geim, and S. Ilani, Imaging hydrodynamic electrons flowing without Landauer–Sharvin resistance, *Nature* **609**, 276 (2022).
 - [8] P. J. W. Moll, P. Kushwaha, N. Nandi, B. Schmidt, and A. P. Mackenzie, Evidence for hydrodynamic electron flow in PdCoO₂, *Science* **351**, 1061 (2016).
 - [9] A. Aharon-Steinberg, T. Völkl, A. Kaplan, A. K. Pariari, I. Roy, T. Holder, Y. Wolf, A. Y. Meltzer, Y. Myasoev, M. E. Huber, B. Yan, G. Falkovich, L. S. Levitov, M. Hücker, and E. Zeldov, Direct observation of vortices in an electron fluid, *Nature* **607**, 74 (2022).
 - [10] P. S. Alekseev, Negative Magnetoresistance in Viscous Flow of Two-Dimensional Electrons, *Phys. Rev. Lett.* **117**, 166601 (2016).
 - [11] G. M. Gusev, A. D. Levin, E. V. Levinson, and A. K. Bakarov, Viscous electron flow in mesoscopic two-dimensional electron gas, *AIP Advances* **8**, 025318 (2018).
 - [12] G. M. Gusev, A. S. Jaroshevich, A. D. Levin, Z. D. Kvon, and A. K. Bakarov, Stokes flow around an obstacle in viscous two-dimensional electron liquid, *Sci. Rep.* **10**, 7860 (2020).
 - [13] Z. T. Wang, M. Hilke, N. Fong, D. G. Austing, S. A. Studenikin, K. W. West, and L. N. Pfeiffer, Nonlinear transport phenomena and current-induced hydrodynamics in ultrahigh mobility two-dimensional electron gas, *Phys. Rev. B* **107**, 195406 (2023).

- [14] J. H. Smet, B. Gorshunov, C. Jiang, L. Pfeiffer, K. West, V. Umansky, M. Dressel, R. Meisels, F. Kuchar, and K. von Klitzing, Circular-Polarization-Dependent Study of the Microwave Photoconductivity in a Two-Dimensional Electron System, *Phys. Rev. Lett.* **95**, 116804 (2005).
- [15] Y. Dai, R. R. Du, L. N. Pfeiffer, and K. W. West, Observation of a Cyclotron Harmonic Spike in Microwave-Induced Resistances in Ultraclean GaAs/AlGaAs Quantum Wells, *Phys. Rev. Lett.* **105**, 246802 (2010).
- [16] A. T. Hatke, M. A. Zudov, L. N. Pfeiffer, and K. W. West, Giant microwave photoresistivity in high-mobility quantum Hall systems, *Phys. Rev. B* **83**, 121301(R) (2011).
- [17] T. Herrmann, I. A. Dmitriev, D. A. Kozlov, M. Schneider, B. Jentzsch, Z. D. Kvon, P. Olbrich, V. V. Bel'kov, A. Bayer, D. Schuh, D. Bougeard, T. Kuczmik, M. Oltcher, D. Weiss, and S. D. Ganichev, Analog of microwave-induced resistance oscillations induced in GaAs heterostructures by terahertz radiation, *Phys. Rev. B* **94**, 081301(R) (2016).
- [18] D. A. Bandurin, K. Kapralov, I. Y. Phinney, K. Lindner, S. Liu, J. H. Edgar, I. A. Dmitriev, P. Jarillo-Herrero, D. Svintsov, and S. D. Ganichev, Cyclotron resonance overtones and near-field magnetoabsorption via terahertz Bernstein modes in graphene, *Nature Physics* **18**, 462 (2022).
- [19] X. Wang, P. Jia, R.-R. Du, L. N. Pfeiffer, K. W. Baldwin, and K. W. West, Hydrodynamic charge transport in an GaAs/AlGaAs ultrahigh-mobility two-dimensional electron gas, *Phys. Rev. B* **106**, L241302 (2022).
- [20] D. Pines and P. M. Nozières, *The Theory of Quantum Liquids* (CRC Press, Boca Raton, FL, 2018).
- [21] P. M. Platzman and P. A. Wolf, *Waves and Interactions in Solid State Plasma* (Academic Press, New York, 1973).
- [22] V. A. Volkov and A. A. Zabolotnykh, Bernstein modes and giant microwave response of a two-dimensional electron system, *Phys. Rev. B* **89**, 121410(R) (2014).
- [23] K. Kapralov and D. Svintsov, Ballistic-to-hydrodynamic transition and collective modes for two-dimensional electron systems in magnetic field, *Phys. Rev. B* **106**, 115415 (2022).
- [24] A. G. Sitenko and K. N. Stepanov, On the Oscillations of an Electron Plasma in a Magnetic Field, *Zh. Exp. Teor. Fiz.* **31**, 642 (1956), [*Sov. Phys. JETP* **4**, 512 (1957)].
- [25] I. B. Bernstein, Waves in a Plasma in a Magnetic Field, *Phys. Rev.* **109**, 10 (1958).
- [26] K. W. Chiu and J. J. Quinn, Plasma oscillations of a two-dimensional electron gas in a strong magnetic field, *Phys. Rev. B* **9**, 4724 (1974).
- [27] I. V. Kukushkin and V. A. Volkov, *Two-dimensional electron liquid in strong magnetic field* (Fizmatkniga, Moscow, 2016).
- [28] P. S. Alekseev and A. P. Alekseeva, Transverse Magnetosonic Waves and Viscoelastic Resonance in a Two-Dimensional Highly Viscous Electron Fluid, *Phys. Rev. Lett.* **123**, 236801 (2019).
- [29] P. S. Alekseev, Magnetosonic Waves in a Two-Dimensional Electron Fermi Liquid, *Semiconductors* **53**, 1367 (2019).
- [30] S. Conti and G. Vignale, Elasticity of an electron liquid, *Phys. Rev. B* **60**, 7966 (1999).
- [31] L. D. Landau and E. M. Lifshitz, *Course of Theoretical Physics: Theory of Elasticity*, Vol. 7 (Pergamon Press, Oxford, 1986).
- [32] L. D. Landau, Oscillations in a Fermi Liquid, *Zh. Exp. Teor. Fiz.* **32**, 59 (1957), [*Sov. Phys. JETP* **5**, 101 (1957)].
- [33] In this work the plain (index-free) notations correspond to interaction renormalized quantities.
- [34] J. Y. Khoo and I. S. Villadiago, Shear sound of two-dimensional Fermi liquids, *Phys. Rev. B* **99**, 075434 (2019).
- [35] J. Y. Khoo, P.-Y. Chang, F. Pientka, and I. Sodemann, Quantum paracrystalline shear modes of the electron liquid, *Phys. Rev. B* **102**, 085437 (2020).
- [36] D. Valentinis, Optical signatures of shear collective modes in strongly interacting Fermi liquids, *Phys. Rev. Res.* **3**, 023076 (2021).
- [37] A. A. Shashkin, S. V. Kravchenko, V. T. Dolgoplov, and T. M. Klapwijk, Sharp increase of the effective mass near the critical density in a metallic two-dimensional electron system, *Phys. Rev. B* **66**, 073303 (2002).
- [38] V. M. Pudalov, M. E. Gershenson, H. Kojima, N. Butch, E. M. Dizhur, G. Brunthaler, A. Prinz, and G. Bauer, Low-Density Spin Susceptibility and Effective Mass of Mobile Electrons in Si Inversion Layers, *Phys. Rev. Lett.* **88**, 196404 (2002).
- [39] S. Anissimova, A. Venkatesan, A. A. Shashkin, M. R. Sakr, S. V. Kravchenko, and T. M. Klapwijk, Magnetization of a Strongly Interacting Two-Dimensional Electron System in Perpendicular Magnetic Fields, *Phys. Rev. Lett.* **96**, 046409 (2006).
- [40] T. Gokmen, M. Padmanabhan, and M. Shayegan, Contrast between spin and valley degrees of freedom, *Phys. Rev. B* **81**, 235305 (2010).
- [41] A. Y. Kuntsevich, Y. V. Tupikov, V. M. Pudalov, and I. S. Burmistrov, Strongly correlated two-dimensional plasma explored from entropy measurements, *Nat. Commun.* **6**, 7298 (2015).
- [42] J. Falson, Y. Kozuka, J. H. Smet, T. Arima, A. Tsukazaki, and M. Kawasaki, Electron scattering times in ZnO based polar heterostructures, *Appl. Phys. Lett.* **107**, 082102 (2015).
- [43] M. Y. Melnikov, A. A. Shakirov, A. A. Shashkin, S. H. Huang, C. W. Liu, and S. V. Kravchenko, Spin independence of the strongly enhanced effective mass in ultra-clean SiGe/Si/SiGe two-dimensional electron system (2023), [arXiv:2304.04272 \[cond-mat.mes-hall\]](https://arxiv.org/abs/2304.04272).
- [44] J. E. Avron, R. Seiler, and P. G. Zograf, Viscosity of Quantum Hall Fluids, *Phys. Rev. Lett.* **75**, 697 (1995).
- [45] J. E. Avron, Odd Viscosity, *J. Stat. Phys.* **92**, 543 (1998).
- [46] P. S. Alekseev, Magnetic resonance in a high-frequency flow of a two-dimensional viscous electron fluid, *Phys. Rev. B* **98**, 165440 (2018).
- [47] P. S. Alekseev and A. P. Alekseeva, Highly viscous electron fluid in GaAs quantum wells (2022), [arXiv:2105.01035 \[cond-mat.mes-hall\]](https://arxiv.org/abs/2105.01035).
- [48] V. P. Silin, Theory of a Degenerate Electron Liquid, *Zh. Exp. Teor. Fiz.* **33**, 495 (1958), [*Sov. Phys. JETP* **6**, 387 (1958)].
- [49] V. P. Silin, The Oscillations of a Degenerate Electron Fluid, *Zh. Exp. Teor. Fiz.* **35**, 1243 (1958), [*Sov. Phys. JETP* **8**, 870 (1959)].
- [50] W. Kohn, Cyclotron Resonance and de Haas-van Alphen Oscillations of an Interacting Electron Gas, *Phys. Rev.* **123**, 1242 (1961).
- [51] A. Klein, D. L. Maslov, L. P. Pitaevskii, and A. V. Chubukov, Collective modes near a Pomeranchuk instability in two dimensions, *Phys. Rev. Research* **1**, 033134 (2019).

- (2019).
- [52] D. Valentinis, J. Zaanen, and D. van der Marel, Propagation of shear stress in strongly interacting metallic Fermi liquids enhances transmission of terahertz radiation, *Sci. Rep.* **11**, 7105 (2021).
- [53] J. P. Eisenstein, L. N. Pfeiffer, and K. W. West, Negative compressibility of interacting two-dimensional electron and quasiparticle gases, *Phys. Rev. Lett.* **68**, 674 (1992).
- [54] J. P. Eisenstein, L. N. Pfeiffer, and K. W. West, Compressibility of the two-dimensional electron gas: Measurements of the zero-field exchange energy and fractional quantum Hall gap, *Phys. Rev. B* **50**, 1760 (1994).
- [55] G. Giuliani and G. Vignale, *Quantum Theory of the Electron Liquid* (Cambridge University Press, 2005).
- [56] L. D. Landau and E. M. Lifshitz, *Course of Theoretical Physics: Electrodynamics of Continuous Media*, Vol. 8 (Pergamon Press, Oxford, 1960).
- [57] R. Aquino and D. G. Barci, Two-dimensional Fermi liquid dynamics with density-density and quadrupolar interactions, *Phys. Rev. B* **100**, 115117 (2019).
- [58] R. Aquino and D. G. Barci, Exceptional points in Fermi liquids with quadrupolar interactions, *Phys. Rev. B* **102**, 201110(R) (2020).